



Pre-braking behaviors analysis based on Hilbert–Huang transform

Bo Wu¹ · Yishui Zhu² · Ran Dong¹ · Kiminori Sato¹ · Soichiro Ikuno¹ · Shoji Nishimura³ · Qun Jin³

Received: 20 November 2022 / Accepted: 21 December 2022 / Published online: 31 December 2022
© The Author(s) 2022

Abstract

Previous studies have shown that about 90% of traffic accidents are due to human error, which means that human factors may affect a driver's braking behaviors and thus their driving safety, especially when the driver makes a braking motion. However, most studies have mounted sensors on the brake pad, ignoring to some extent an analysis of the driver's behavior before the brake pad is pressed (pre-braking). Therefore, to determine the effect of different human factors on drivers' pre-braking behaviors, this study focused on analyzing drivers' local joints (knee, ankle, and toe) by a motion capture device. A Hilbert–Huang Transform (HHT)-based local human body movement analysis method was used to decompose the realistic complex pre-braking actions into sub-actions such as intrinsic mode functions (IMF1, IMF2, etc.). Analysis of the results showed that IMF1 is a common and necessary action when pre-braking for all drivers, and IMF2 may be the safety assurance action that allows right-foot transverse movement at the beginning part of the pre-braking process. We also found that the experienced, male, and Phys.50 groups may have consistent characteristics in the HHT scheme, which could mean that such drivers would have better performance and efficiency during the pre-braking process. The results of this study will be useful in decomposing and discerning the specific actions that lead to accidents, providing insights into driver training for novice drivers, and guiding the construction of daily automated driver assistance or accident prevention systems (advanced driver assistance systems, ADASs).

Keywords Hilbert–Huang Transform · Empirical Mode Decomposition · Motion Measurement · Vehicle Driving · Braking Behaviors Analysis · Driver Characteristics Analysis

✉ Ran Dong
randong@stf.teu.ac.jp

Bo Wu
wubo@stf.teu.ac.jp

Yishui Zhu
yszhu@chd.edu.cn

Kiminori Sato
satohkmn@stf.teu.ac.jp

Soichiro Ikuno
ikuno@stf.teu.ac.jp

Shoji Nishimura
kickaha@waseda.jp

Qun Jin
Jin@waseda.jp

¹ School of Computer Science, Tokyo University of Technology, 1404-1 Katakuramachi, Hachioji City, Tokyo, Japan

² Department of Software Engineering, School of Information Engineering, Chang'an University, Xi'an, China

³ Faculty of Human Sciences, Waseda University, Tokorozawa, Japan

1 Introduction

The number of private cars continues to grow, and traffic accidents have become one of the most serious social problems in the world (Rongqiang et al. 2016). About 90% of traffic accidents are due to human causes (NHTSA 2002). In particular, drivers' braking-related behaviors are considered to be an important cause of accidents (Ren et al. 2011). For example, some inexperienced drivers may use the gas pedal instead of the brake and cause an accident (Schmidt et al. 1997).

According to our previous studies (Wu et al. 2020b) and related research (Lyu et al. 2017, 2018; Hault-Dubrulle et al. 2011), drivers' experience, gender, and physique as human factors may affect a driver's braking behavior and thus his driving safety. However, most studies have mounted sensors on the brake pad. Only a few studies (Stahl et al. 2014; Hou et al. 2019) focused on the analysis of driver's behavior pre-braking, but they used inconsistent definitions that differed

Table 1 Related studies about braking

References	Conditions	Factors	Algorithm	Data collection
Tu et al. (2015)	Visibility/weather	Reaction time, maximum deceleration rate, mean deceleration rate, maximum brake pedal force, mean brake pedal force	Significance test	0-Dof and 8-Dof driving simulators
Li et al. (2017)	Signalized intersection	Braking frequency, stopping distance	Braking assistance algorithm	Field test
Wu et al. (2018)	Urgency of emergency scenario	Braking response time, braking deceleration, braking deceleration jerk	Statistical analysis	China naturalistic driving data (China-FOT)
Xiao et al. (2019)	Braking of automobile in front/Road-blocks cutting off other lanes/Simulated in a real road environment	Automobile velocity, braking velocity, sustained action time	Fuzzy aggregation analysis, fuzzy probabilistic neural network	From a professional testing ground
Li et al. (2020)	Emergency braking of vehicle in front under a connected vehicle environment	Speed control intensity	Spatiotemporal diagram, curvature index	AutoSim:AS simulation platform
Pawar et al. (2020)	Increasing time pressure condition	Brake pedal force, brake-to-maximum brake (BTMB) transition time	Statistical analysis	Driving simulator
Zhu et al. (2021)	Typical vehicle-following braking condition	Speed, deceleration, distance, etc	k-means, particle swarm optimization, SVM, genetic algorithm	Ebooster

from this paper (i.e., driver's body actions before the brake pad are pressed).

Therefore, an in-depth analysis of driver pre-brake-related behaviors is necessary to determine the relationship between various human factors and possible traffic accidents.

With the advancement of sensors and Internet of Things (IoT) technology, human in-vehicle behavior can already be collected and analyzed with great accuracy. Among them, an accelerometer-based motion capture device to record the subject's whole-body movements can be applied to many different scenarios (Wu et al. 2020a). A dedicated kit with acceleration sensors and similar devices to capture motion can collect data on the subject's body movements with high accuracy, even outside of a laboratory environment.

Moreover, based on the collected human body movements data, motion features with different action purposes can be decomposed in the frequency domain (Winter 2009). Thus, to facilitate the analysis of the similarities and differences between actions, action frequency analysis in previous studies has mainly used Fourier transform (Bruderlin and Williams 1995) and wavelet transform (Aminian and Najafi 2004), which are not suitable for decomposing human actions due to interpretation difficulties.

Therefore, based on a set of experiments performed at a vehicle test field, this study focused on analyzing drivers' pre-braking actions and tried to propose an action decomposition-based local human body movement analysis method to discover similarities and differences in pre-braking actions among drivers with different driving experience, gender, and physique. The motion capture device called Xsens MVN Animate (Xsens 2022) was used for the data collection. Unlike traditional motion capture instruments, MVN can additionally collect human joint data, such as for spinal joints and toes, to calculate more joint angles to represent the subject's posture for motion analysis. Based on related joint angle calculations, an action decomposition method, such as Hilbert–Huang Transform (HHT), is applied to analyze the pre-braking actions in the instantaneous frequency domain. The HHT method is a kind of empirical decomposition, which can better decompose the realistic complex actions of human beings through nonlinear decomposition.

The results of this study will be useful in decomposing and discerning the specific actions that lead to accidents, providing insights into driver training for novice drivers, and guiding the construction of daily automated driver assistance or accident prevention systems (advanced driver assistance systems, ADASs).

The remainder of this paper is organized as follows: an overview of related studies on driver behaviors analysis, braking motion analysis, and Hilbert–Huang Transform will be provided in Sect. 2. In Sect. 3, the methodology, related measures definitions, and description of the dataset will be provided. Then, the experimental design, dataset,

Fig. 1 The pre-braking behaviors in this study

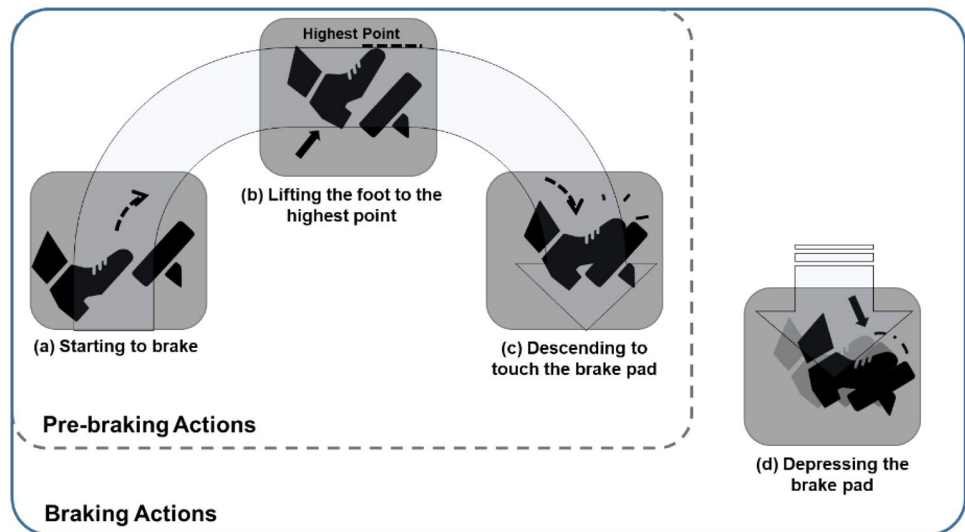


Fig. 2 The Xsens MVN motion capture device



analysis results, and discussion will be provided in Sects. 4 and 5. Finally, we will summarize the research results and provide our perspective regarding promising future research in Sect. 6.

2 Related studies and hypotheses

2.1 Driver behaviors analysis

Most research has focused on driver behaviors to improve the safety of driving performance. For example, Cao et al. (2014) modeled the cognitive architecture underlying drivers' skills and supported quantitative simulation of the driving behavior. Jia et al. (2020) analyzed different driving styles, including extreme acceleration and emergency

braking behavior and other behaviors by using long short-term memory and convolutional neural network methods. Driving data metrics show that there is no specific time point after which driving behavior stabilizes for all drivers (Stavarakaki et al. 2020). However, Lodha et al. (2021) showed that the braking time in chronic stroke disease survivors was longer than in other groups. Nugroho et al. (2021) predicted the remaining age of brake lining by studying various driving behaviors and braking power. In summary, although there are many studies about driver behaviors, braking behaviors, and braking time, few are related to pre-braking behaviors.

Table 2 Details of calculated measures for analysis

No	Name of Joint
1	Pelvis
2	L5
3	L3
4	T12
5	T8
6	Neck
7	Head
8	Right Shoulder
9	Right Upper Arm
10	Right Forearm
11	Right Hand
12	Left Shoulder
13	Left Upper Arm
14	Left Forearm
15	Left Hand
16	Right Upper Leg
17	Right Lower Leg
18	Right Foot
19	Right Toe
20	Left Upper Leg
21	Left Lower Leg
22	Left Foot
23	Left Toe

2.2 Braking motion analysis and pre-braking behavior

Braking is a common manipulation during the driving process, and it is most related to traffic accidents. Proper braking behavior can keep driving safe and comfortable for

the beings in the vehicle. Many researchers have analyzed the braking behaviors in some urgent scenarios related to potential accidents (Wu et al. 2018; Li et al. 2020; Pawar et al. 2020). Moreover, other researchers studied the braking actions in usual driving environments (Tu et al. 2015; Li et al. 2017; Xiao et al. 2019; Zhu et al. 2021). Most of the research investigated braking as a whole process but did not focus on pre-braking separately.

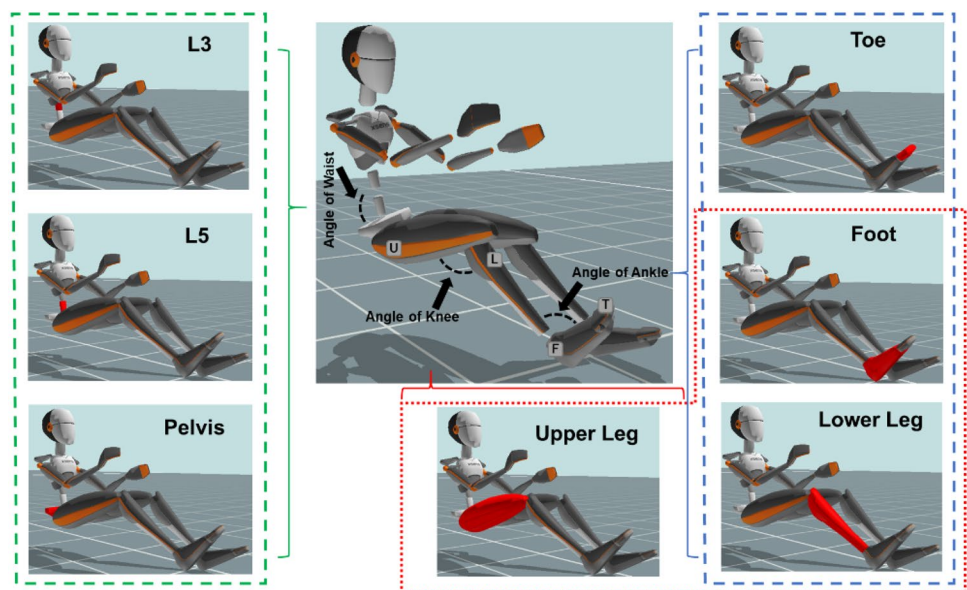
In summary, Table 1 shows that related studies have focused more on the accident itself, with the driver’s pre-braking action usually studied as one of the main maneuvers to avoid a collision. Not much research has been done on everyday driving behaviors, such as turning and stopping, with respect to pre-braking.

Furthermore, different studies used different definitions for pre-braking behaviors. For example, some studies defined the braking action as the action of slowing down when encountering an accident (Susumu et al. 2009).

Therefore, in this paper, we define “pre-braking behaviors” as the action behaviors exhibited by a driver’s foot before it touches the brake pedal during a whole braking action.

As shown in Fig. 1, the entire braking behavior of the driver’s right foot is divided into four stages: (a) starting to brake, (b) lifting the foot to the highest point, (c) descending to touch the brake pad, and (d) depressing the brake pad. Therefore, the “pre-braking behaviors” are defined as actions (a) to (c). Because action (d) has been extensively studied by previous research, this paper will not focus on it.

Fig. 3 The angles for calculation



2.3 The xsens MVN motion capture device

As shown in Fig. 2, the high precision accelerometer-based motion capture device named Xsens MVN (Troje 2002) was used in this study to collect the data on drivers’ body movements. Xsens MVN can record the 3D coordinates of a subject’s joints at a frequency of once every 4 ms. As a wearable motion capture system, unlike traditional camera-based motion capture devices, Xsens MVN can provide continuous data recording services including the outdoor situation by connecting a battery-operated dedicated recording device.

The MVN has 17 wearable ultra-small trackers that are designed to withstand high impacts such as rolls and stunts. In contrast to traditional motion capture devices, the Xsens MVN device can collect data on 23 joints including spinal segments T12, T8, L5, L3, and toes as XML files with high precision. The details of the collectible joint data are shown in Table 2.

2.4 Hilbert–Huang transform

Hilbert–Huang Transform is applied to analyze and generate motion data collected by motion capture systems due to its high performance in dealing with nonlinear data in the instantaneous frequency domain. Dong et al. (2020b) proposed a framework to analyze human captured motions using HHT based on multivariate empirical mode decomposition (MEMD). The previous research revealed that a common human action could be decomposed into multiple sub-actions with different purposes. For example, decomposed high-frequency sub-actions could be removed by HHT to achieve motion smoothing for robot motors (Dong et al. 2020a). Using these decomposed multiple sub-actions, Dong et al. (2021) also presented a method to generate realistic motion features for robot motion design, which demonstrated that HHT could provide motion training data for deep learning.

In summary, previous research showed that HHT could be adopted in human motion analysis and editing. However, different human actions contain distinct motion features and multiple sub-actions, according to the biomechanical mechanism of the human body structure (Winter 2009). Thus, it is necessary to perform an in-depth analysis of distinct human actions, such as pre-braking actions using statistical methods.

3 Methodology

3.1 Angle calculation of key joints

The MVN motion capture device used in this study can support the acquisition of coordinate data for a total of 23 joints

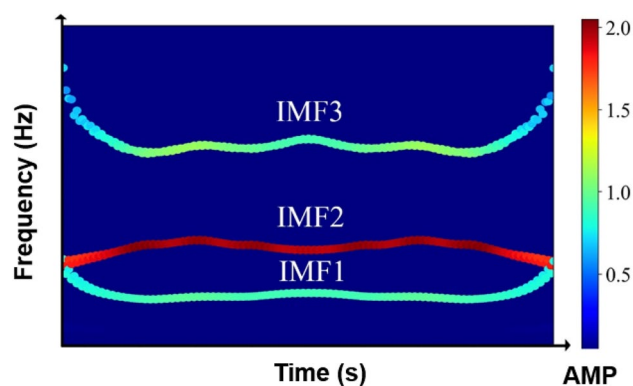


Fig. 4 An example Hilbert spectrum

in the whole body (Troje 2002). In order to better represent the driver's movements during the pre-braking action, as shown in Fig. 3, this study focused on three joint angles related to braking behaviors: the waist, right knee, and right ankle. Therefore, because an aimed angle needs to be calculated from the coordinates of three joints, the following data for seven joints were analyzed: pelvis, spinal joints L3 & L5, right upper leg, right lower leg, right foot, and right toe tip.

Specifically, for the calculation of the knee angle, we can take the coordinates of the three joints, upper leg $U (X_u, Y_u, Z_u)$, lower leg $L (X_l, Y_l, Z_l)$, and foot $F (X_f, Y_f, Z_f)$ and calculate the angle of knee θ_k by Eq. (1):

$$\theta_k = \arccos \frac{\overline{LU} \times \overline{LF}}{|\overline{LU}| \times |\overline{LF}|} \tag{1}$$

where the vectors \overline{LU} and \overline{LF} can be obtained by Eqs. (2) and (3):

$$\overline{LU} = (X_u - X_l, Y_u - Y_l, Z_u - Z_l) \tag{2}$$

$$\overline{LF} = (X_f - X_l, Y_f - Y_l, Z_f - Z_l) \tag{3}$$

Finally, the driver’s three joint angles include the angle of knee θ_k , angle of ankle θ_a , and angle of waist θ_w can be calculated. By analyzing the changes of these three joint angles, we can gain a description of the driver's relevant actions during pre-braking.

3.2 Hilbert–Huang transform

The Hilbert–Huang transform (HHT) is a process of empirical mode decomposition (EMD) of the original signal that applies the Hilbert Transform (HT) to each decomposed frequency component. Because HHT decomposes signals nonlinearly, it can achieve better results when analyzing nonlinear and nonstationary motion capture data than

Fig. 5 Map of the CAV test field

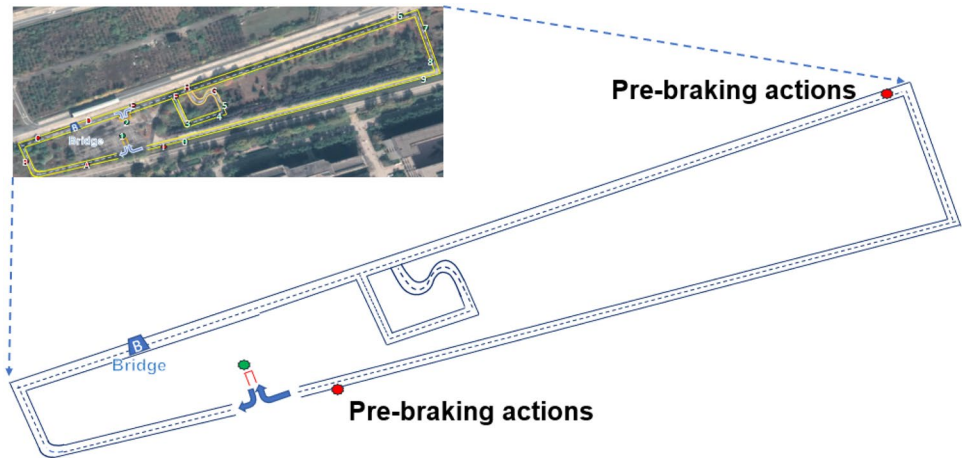


Table 3 Specific demographic information about the subjects

No	Gender	Driving Experience	Months of Driving Experience	Knee Height (cm)
1	Female	Novice	0	50
2	Male	Novice	0	50
3	Male	Novice	0	55
4	Male	Experienced	306	50
5	Male	Experienced	180	55
6	Female	Novice	36	50
7	Male	Experienced	180	45
8	Female	Experienced	120	50
9	Male	Experienced	216	45
10	Female	Novice	0	50

other methods such as short-time Fourier transform (STFT) (Huang and Shen 2014).

An analytic signal $z(t)$ is defined as Eq. (4) in the complex plane, where $z_r(t)$ is the real part observed in the real world, and $z_i(t)$ is the imaginary part calculated by HT (Bracewell 1978).

$$z(t) = z_r(t) + iz_i(t) \tag{4}$$

As shown in Eq. (5), HT transforms the real part $z_r(t)$ into its imaginary part $z_i(t)$ by considering the observed signal $z_r(t) = A(t) \cos(\omega(t)t)$ (Bracewell 1978).

$$z_i(t) = \frac{1}{\pi} \text{PV} \int_{-\infty}^{+\infty} \frac{z_r(\tau)}{t - \tau} d\tau = \frac{1}{\pi t} * z_r(t) \tag{5}$$

After the real part $z_r(t)$ and imaginary part $z_i(t)$ of $z(t)$ are obtained, the instantaneous amplitude (AMP) $A(t)$ and frequency $\omega(t)$ are calculated according to Eq. (6).

$$A(t) = \sqrt{z_r^2(t) + z_i^2(t)}, \omega(t) = \frac{d}{dt} \tan^{-1} \frac{z_i(t)}{z_r(t)} \tag{6}$$

However, as we can see from the definition of HT, only monochromatic wave signals, that is, only $A(t) \cos(\omega(t)t)$, can be transformed by HT to calculate its imaginary part. Consequently, the instantaneous AMP and frequency of a composite wave made of distinct monochromatic waves cannot be obtained correctly. Meanwhile, because human motion data is not a monochromatic signal, HT is not satisfied by adopting nonlinear and nonstationary data such as motion capture data.

To deal with this issue, Huang and Shen (2014) provided a method called empirical mode decomposition (EMD), empirically decomposing a composite wave consisting of multiple monochromatic waves into a finite number of pseudo monochromatic waves, a so-called intrinsic mode function (IMF), and a residual without any frequency component, a so-called trend. Equation (7) demonstrates that an observed signal $x(t)$ is decomposed into several IMFs $c_i(t)$ and a trend $r(t)$.

$$x(t) = \sum_{i=1}^n c_i(t) + r(t) \tag{7}$$

The definition of IMF is as follows:

- (1) The number of extremes is equal to the number of zero crossings, or the difference between them is 1.
- (2) At any given time, the average of the envelopes connecting the maximum and minimum values is zero.

Based on the definition above, IMF is extracted from high frequency to lower frequency using an algorithm (Huang and Shen 2014). Then, the trend is the residual with no frequency component after extracting all IMFs. Because the IMF satisfies the HT assumption, after decomposing nonlinear and nonstationary data into IMFs, we can let $z_r(t) = c_i(t)$ to obtain $z_i(t)$ by Eq. (5). Then, the instantaneous AMP and frequency can be obtained correctly by Eq. (6) for each IMF.

To demonstrate how IMFs are shown in the instantaneous frequency domain, we used an artificial signal $s(t)$ consisting of three monochromatic waves, Eq. (8), as an example of Hilbert spectral analysis (HSA). Please note that we used this example only to demonstrate HSA. Thus, for simplicity, the three monochromatic waves in artificial signal $s(t)$ are stationary with constant frequency, while motion data are nonstationary with variable frequency.

$$s(t) = \sin\left(\frac{\pi t}{10}\right) + 2\sin\left(\frac{\pi t}{20}\right) + \cos\left(\frac{\pi t}{40}\right) \tag{8}$$

Figure 4 shows the instantaneous AMP and frequencies of all decomposed IMFs obtained by HT. The results are displayed in time on the horizontal axis, frequency on the vertical axis, and AMPs are presented by color.

In this paper, we numbered the index of each IMF from low frequency to high frequency. Thus, IMF1 corresponds to $\cos(\frac{\pi t}{40})$, IMF2 corresponds to $2\sin(\frac{\pi t}{20})$, and IMF3 corresponds to $\sin(\frac{\pi t}{10})$. Using the HSA, we can analyze pre-braking actions by decomposing angle of knee θ_k , angle of ankle θ_a , and angle of waist θ_w , and calculate their instantaneous frequency and AMP for statistical analysis.

In addition, many studies have been conducted to extend the EMD from univariate to multivariate, expanding the range of applications of the HHT (Rehman and Mandic 2010). Therefore, in this study, we focused on the multi-channel of motion capture data in pre-braking actions and applied the MEMD to decompose the pre-braking actions into multivariate IMF signals.

As can be seen from the definition of EMD, HHT differs in principle from Fourier transform (FT). FT linearly decomposes a signal into monochromatic waves based on

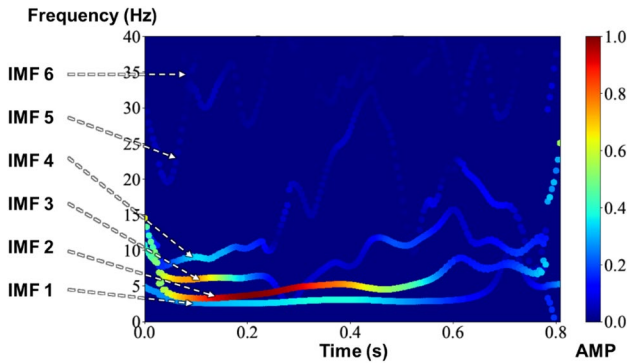


Fig. 6 Different action modes from the pre-braking behaviors

Table 4 The measures using for analysis

No	Measure	Abb	Description
1	Waist freq. 1	Wf1	Average IMF 1 frequency for waist
2	Knee freq. 1	Kf1	Average IMF 1 frequency for knee
3	Ankle freq. 1	Af1	Average IMF 1 frequency for ankle
4	Waist amp. 1	Wa1	Average IMF 1 amplitude for waist
5	Knee amp. 1	Ka1	Average IMF 1 amplitude for knee
6	Ankle amp. 1	Aa1	Average IMF 1 amplitude for ankle
7	Waist freq. 2	Wf2	Average IMF 2 frequency for waist
8	Knee freq. 2	Kf2	Average IMF 2 frequency for knee
9	Ankle freq. 2	Af2	Average IMF 2 frequency for ankle
10	Waist amp. 2	Wa2	Average IMF 2 amplitude for waist
11	Knee amp. 2	Ka2	Average IMF 2 amplitude for knee
12	Ankle amp. 2	Aa2	Average IMF 2 amplitude for ankle
13	Waist freq. sd 1	Wfs1	Standard variance of IMF 1 frequency for waist
14	Knee freq. sd 1	Kfs1	Standard variance of IMF 1 frequency for knee
15	Ankle freq. sd 1	Afs1	Standard variance of IMF 1 frequency for ankle
16	Waist amp. sd 1	Was1	Standard variance of IMF 1 amplitude for waist
17	Knee amp. sd 1	Kas1	Standard variance of IMF 1 amplitude for knee
18	Ankle amp. sd 1	Aas1	Standard variance of IMF 1 amplitude for ankle
19	Waist freq. sd 2	Wfs2	Standard variance of IMF 2 frequency for waist
20	Knee freq. sd 2	Kfs2	Standard variance of IMF 2 frequency for knee
21	Ankle freq. sd 2	Afs2	Standard variance of IMF 2 frequency for ankle
22	Waist amp. sd 2	Was2	Standard variance of IMF 2 amplitude for waist
23	Knee amp. sd 2	Kas2	Standard variance of IMF 2 amplitude for knee
24	Ankle amp. sd 2	Aas2	Standard variance of IMF 2 amplitude for ankle

mathematical proof. In contrast, EMD empirically decomposes the signal into pseudo monochromatic waves, IMFs, with variable frequency and AMP. Therefore, HHT is more beneficial for analyzing pre-braking actions that are nonlinear and nonstationary motion capture data.

Table 5 Basic statistics for HHT method results

Measure	N	Range	Mean		Std deviation
			statistic	Std. Error	
Wf1	100	11.19	3.80	0.26	2.64
Kf1	100	13.49	3.21	0.23	2.29
Af1	100	13.73	3.14	0.24	2.36
Wa1	100	0.27	0.05	0.00	0.04
Ka1	100	2.30	0.42	0.05	0.47
Aa1	100	8.99	1.30	0.14	1.41
Wf2	51	3.20	4.18	0.11	0.81
Kf2	51	3.71	3.50	0.12	0.84
Af2	51	3.82	3.30	0.12	0.82
Wa2	51	0.12	0.04	0.00	0.02
Ka2	51	0.45	0.17	0.02	0.11
Aa2	51	1.43	0.45	0.05	0.38
Wfs1	100	15.34	3.99	0.29	2.87
Kfs1	100	15.64	3.58	0.30	2.98
Afs1	100	12.51	3.24	0.25	2.52
Was1	100	0.08	0.02	0.00	0.02
Kas1	100	1.08	0.19	0.02	0.18
Aas1	100	3.42	0.62	0.06	0.63
Wfs2	51	8.45	4.14	0.26	1.89
Kfs2	51	6.17	4.00	0.21	1.48
Afs2	51	9.46	4.11	0.28	1.97
Was2	51	0.07	0.02	0.00	0.02
Kas2	51	0.42	0.16	0.02	0.11
Aas2	51	1.94	0.45	0.06	0.40

Table 6 Amount of data for the IMF2

Measure	N (Total)						
	Experienced (48)	Novice (52)	Male (57)	Female (43)	Phys.45 (18)	Phys.50 (65)	Phys.55 (17)
Wf2/Wfs2	28	23	31	20	9	32	10
Kf2/Kfs2	28	23	31	20	9	32	10
Af2/Afs2	28	23	31	20	9	32	10
Wa2/Was2	28	23	31	20	9	32	10
Ka2/Kas2	28	23	31	20	9	32	10
Aa2/Aas2	28	23	31	20	9	32	10

4 Experiments and dataset

4.1 Experiments

To obtain the target data, we conducted a set of driving experiments at Chang'an University, on the Connected and Automated Vehicle (CAV) Test Field, located in Xi'an, China in September 2019. A general civilian car (Volkswagen Sagitar, Automatic/1.6 L/3-box/5 seats) was used for the experiments. The steering wheel of the experimental vehicle was on the left side. As shown in Fig. 5, the CAV test field was oval-shaped, and all subjects were required to start at the green point (garage), drive clockwise for one lap, and then stop and reenter the garage. All subject drivers were asked to perform their usual driving in the test site while wearing the MVN motion capture device.

This research focused on the driving movements before the driver turned right (right angle) and during parking (red points) where braking actions were certain to occur. Statistically, the average speed of the driver at the time of reaching the red point was 20 km/s. Some red balloons were set at the roadside to remind the driver to perform the relevant actions, but the specific operation was entirely up to the driver to perform according to daily habits (no verbal instruction). The starting time of the data used for analysis was determined based on the driver's foot movements.

Drivers' physical data including knee height, ankle height and shoe length, etc. were collected before the main experiments to increase the accuracy of the collected data. On the other hand, being difficult to wear, this experiment did not use the sensor carrier suit of Xsens MVN Animate. Instead, a more convenient vest carrier suit from the Xsens Awinda is used.

As shown in Table 3, a total of 10 drivers with different driving experiences, genders, and physiques were invited to participate in the experiments, including five taxi drivers, four university students, and one university teacher. Because one's knee height is correlated with one's stature (RxKinetics 2020), knee height was used as a variable to differentiate

Table 7 Results of Mann–Whitney *U* tests for driving experience (average data)

Measure	Driving exp	<i>N</i>	Mean rank	<i>U</i>	<i>W</i>	<i>Z</i>	<i>p</i>	Effect size
Wf1	Novice	52	49.1	1175	2553	−0.504	0.615	−0.050
	Experienced	48	52.02					
Kf1	Novice	52	54.60	1035	2211	−1.47	0.142	−0.147
	Experienced	48	46.06					
Af1*	Novice	52	56.79	921	2097	−2.256	0.024	−0.226
	Experienced	48	43.69					
Wa1	Novice	52	51.17	1213	2389	−0.241	0.809	−0.024
	Experienced	48	49.77					
Ka1	Novice	52	54.13	1059	2235	−1.304	0.192	−0.130
	Experienced	48	46.56					
Aa1	Novice	52	53.42	1096	2272	−1.049	0.294	−0.105
	Experienced	48	47.33					
Wf2	Novice	23	24.22	281	557	−0.776	0.438	−0.109
	Experienced	28	27.46					
Kf2	Novice	23	29.65	238	644	−1.59	0.112	−0.223
	Experienced	28	23.00					
Af2	Novice	23	29.78	235	641	−1.647	0.100	−0.231
	Experienced	28	22.89					
Wa2	Novice	23	23.30	260	536	−1.174	0.241	−0.164
	Experienced	28	28.21					
Ka2	Novice	23	27.00	299	705	−0.435	0.663	−0.061
	Experienced	28	25.18					
Aa2	Novice	23	26.48	311	717	−0.208	0.835	−0.029
	Experienced	28	25.61					

‡*p*-value < 0.1**p*-value < 0.05

physiques. The group with extensive driving experience had driven an average distance of more than 1000 km, and the novice drivers were basically students who just got their licenses, which means they almost did not have any practical driving experience. Statistically, the average age of experienced drivers was 42.4 years, and the average age of novice drivers was 24.6 years. All subjects were in good health and were asked to perform 10 experiments each. No additional instructions were given by the data recording staff during the experiment.

4.2 Dataset selection and pre-processing

Based on the pre-processing, a total of 100 sets of driving data of pre-braking actions (including whole-body joint coordinates, speed, moving distance, etc.) were selected for the following movement decomposing via the HHT method. Finally, the aimed measures were calculated for each data set, including the action trend, the standard variance of all IMFs' frequency and AMP for drivers' waist, knee, and ankle during the pre-braking actions.

The traditional HHT method mainly focuses on the decomposition of whole-body movements, which means a large amount of redundant data needs to be processed before the main analysis. In this paper, according to the characteristics of the target joints' movement, we innovatively established a method for local movements decomposition and analysis. This meant that instead of disassembling the whole-body movements directly, in order to calculate the joint angle changes, we disassembled only the selected key joints' changing movements into different sub-actions for the analysis.

Specifically, based on the key joints calculation and HHT method mentioned above, the drivers' pre-braking actions for their "body–right leg" part (waist, knee, and ankle) were decomposed into different sub-actions by the motion data's frequency.

As shown in Fig. 6, through a pre-analysis, a set of braking actions can be decomposed into many sets of IMFs according to the frequency, which can be numbered according to frequency as IMF 1–6. A larger IMF number (e.g., IMF 6) indicates a higher frequency of the action performed by the subject.

Table 8 Results of Mann–Whitney *U* tests for experiences (standard variance data)

Measure	Driving exp	<i>N</i>	Mean Rank	<i>U</i>	<i>W</i>	<i>Z</i>	<i>p</i>	Effect size
Wfs1	Novice	52	52.06	1167	2343	−0.559	0.576	−0.056
	Experienced	48	48.81					
Kfs1	Novice	52	48.58	1148	2526	−0.690	0.490	−0.069
	Experienced	48	52.58					
Afs1	Novice	52	50.02	1223	2601	−0.172	0.863	−0.017
	Experienced	48	51.02					
Was1	Novice	52	47.44	1089	2467	−1.097	0.273	−0.110
	Experienced	48	53.81					
Kas1‡	Novice	52	45.83	1005	2383	−1.677	0.094	−0.168
	Experienced	48	55.56					
Aas1	Novice	52	46.52	1041	2419	−1.428	0.153	−0.143
	Experienced	48	54.81					
Wfs2	Novice	23	28.09	274	680	−0.909	0.364	−0.127
	Experienced	28	24.29					
Kfs2*	Novice	23	19.43	171	447	−2.858	0.004	−0.400
	Experienced	28	31.39					
Afs2	Novice	23	23.65	268	544	−1.022	0.307	−0.143
	Experienced	28	27.93					
Was2	Novice	23	22.35	238	514	−1.590	0.112	−0.233
	Experienced	28	29.00					
Kas2*	Novice	23	20.57	197	473	−2.366	0.018	−0.331
	Experienced	28	30.46					
Aas2	Novice	23	24.52	288	564	−0.644	0.520	−0.090
	Experienced	28	27.21					

‡*p*-value < 0.1**p*-value < 0.05

However, based on previous studies (Thorpe et al. 1996), when converting frequency to seconds, if the time of an IMF is less than 0.1 s, then the subject has no control over it, which means that it can be considered a noise action. Therefore, in this paper, only IMFs with a time greater than 0.1 s after conversion are discussed.

The AMP of each IMF can also be obtained and represented in different colors. The closer the color is closer to red, the greater the AMP. A stronger AMP represents a greater change of joint angle, which means a greater use of force.

In this research, in order to distinguish the actions represented by different IMFs and to analyze the differences between different groups of subjects, we converted the graph-based data to row data and pre-processed them. Because their frequency/AMP fluctuates with time, except the average value, we also converted the IMF data into computable values by taking the standard variance.

Therefore, because only IMF 1 and 2 were eligible (> 0.1 s) in our data set, the measures shown in Table 4 were used for the following inter-group comparative analysis.

5 Analysis results and discussion

To compare the similarities and differences in pre-braking actions between drivers with different experience, gender, and physique, this section will discuss the results both statistically and graphically.

5.1 Statistics-based comparative analysis

As the first step, the values of the quantity, range, standard deviation, and standard error, etc. of the data were confirmed using basic statistics (Table 5).

Table 9 Results of Mann–Whitney U tests for genders (average data)

Measure	Gender	N	Mean rank	U	W	Z	p	Effect size
Wf1	Female	43	51.05	1202	2855	−0.164	0.870	−0.016
	Male	57	50.09					
Kf1	Female	43	55.21	1023	2676	−1.410	0.159	−0.141
	Male	57	46.95					
Af1‡	Female	43	56.84	953	2606	−1.897	0.058	−0.190
	Male	57	45.72					
Wa1	Female	43	53.91	1079	2732	−1.020	0.308	−0.102
	Male	57	47.93					
Ka1*	Female	43	61.98	732	2385	−3.436	0.001	−0.344
	Male	57	41.84					
Aa1	Female	43	54.77	1042	2695	−1.278	0.201	−0.128
	Male	57	47.28					
Wf2	Female	20	25.15	293	503	−0.328	0.743	−0.046
	Male	31	26.55					
Kf2	Female	20	27.15	287	783	−0.444	0.657	−0.062
	Male	31	25.26					
Af2	Female	20	30.05	229	725	−1.563	0.118	−0.219
	Male	31	23.39					
Wa2	Female	20	24.15	273	483	−0.714	0.475	−0.100
	Male	31	27.19					
Ka2*	Female	20	32.1	188	684	−2.354	0.019	−0.330
	Male	31	22.06					
Aa2	Female	20	27.7	276	772	−0.656	0.512	−0.092
	Male	31	24.9					

‡p-value < 0.1

*p-value < 0.05

As shown in Table 5, the basic statistical results showed that all results had the first layer of IMF (IMF1), but only a portion of the data had the second layer of IMF (IMF2). Because the different levels of IMF layers represent different sub-actions, it was necessary to investigate the characteristics of the data that had IMF2. Therefore, the data related to IMF2 were counted separately according to different driving experience, gender, and physique before the analysis.

As shown in Table 6, the amount of data for IMF2 was relatively balanced when grouped by driving experience and gender. However, when grouped by physique (knee height), the amount of data for the Phys.50 group was higher than the other two groups by almost three times. This may represent a higher probability that subjects in the Phys.50 group will perform the sub-action represented by IMF2 relative to the other groups.

Therefore, to explain the findings, we compared the differences in detail for IMF1 and IMF2 values among the different groups, which were classified by driving experience, gender, and physique.

5.1.1 Differences between drivers with different driving experience

According to the preprocessing of row data by Kolmogorov–Smirnov Normality Test, we determined that the results did not conform to a normal distribution. Therefore, to compare the differences in pre-braking actions exhibited by subjects with different driving experience, the two types of data (average and standard variance data for IMF1 and IMF2 frequency and AMP) were analyzed using independent-samples Mann–Whitney U tests.

For the average data, as shown in Table 7, significant differences ($p < 0.05$) were identified only for the indicators Af1 of IMF1, which means that the experienced drivers had a lower speed of ankle joint movement change for sub-action IMF1.

For the standard variance data, as shown in Table 8, no significant differences ($p < 0.05$) were identified for all indicators of IMF1, which means that for drivers with different driving experience, there was no difference in their

Table 10 Results of Mann–Whitney U tests for genders (standard variance data)

Measure	Gender	N	Mean rank	U	W	Z	p	Effect size
Wfs1	Female	43	51.09	1200	2853	−0.178	0.859	−0.018
	Male	57	50.05					
Kfs1	Female	43	50.67	1218	2871	−0.052	0.958	−0.005
	Male	57	50.37					
Afs1	Female	43	51.35	1189	2842	−0.254	0.799	−0.025
	Male	57	49.86					
Was1	Female	43	49.35	1176	2122	−0.345	0.73	−0.035
	Male	57	51.37					
Kas1	Female	43	54.12	1070	2723	−1.083	0.279	−0.108
	Male	57	47.77					
Aas1	Female	43	45.42	1007	1953	−1.521	0.128	−0.152
	Male	57	54.33					
Wfs2	Female	20	29.65	237	733	−1.408	0.159	−0.1972
	Male	31	23.65					
Kfs2	Female	20	23.95	269	479	−0.791	0.429	−0.1108
	Male	31	27.32					
Afs2‡	Female	20	21.6	222	432	−1.698	0.09	−0.2378
	Male	31	28.84					
Was2‡	Female	20	21.5	220	430	−1.736	0.083	−0.2431
	Male	31	28.9					
Kas2	Female	20	26.2	306	802	−0.077	0.938	−0.0108
	Male	31	25.87					
Aas2	Female	20	22.65	243	453	−1.293	0.196	−0.1811
	Male	31	28.16					

‡ p -value < 0.1* p -value < 0.05

first sub-action (IMF1)'s frequency or AMP during the pre-braking action. However, unlike the results of IMF1, a significant difference was identified for measure Kfs2 and Kas2 from IMF2 ($p < 0.05$). This result indicates that in the group of subjects who performed the IMF2 sub-action, the experienced drivers did the IMF2 action with a greater knee vibration in both frequency and AMP than the novice drivers.

5.1.2 Differences between drivers of different genders

Next, to compare the differences in pre-braking actions exhibited by subjects of different gender, independent-samples Mann–Whitney U tests were used to analyze the data of IMF1 and IMF2's frequency and AMP.

For the average data, as shown in Table 9, significant differences ($p < 0.05$) were identified for the indicators Ka1 of IMF1 and Ka2 of IMF2, and significant differences ($p < 0.1$) were identified for the indicator Af1, which means that the male drivers had a lower force on their knee joint for both sub-actions IMF1 and IMF2, and the male drivers may also

have had a lower speed of their ankle joint movement change for sub-action IMF1. The results for Af1 and Ka2 were very similar to the results in Sect. 5.1.1 for the differences between drivers with different driving experience.

For the standard variance data, as shown in Table 10, although there was a significant difference at $p < 0.1$ for the Afs2 and Was2 measures of IMF2, there was no significant difference at $p < 0.05$ for all indicators. This means that for drivers with different gender, there was no difference in either sub-action (IMF1 and IMF2)'s frequency or AMP during the pre-braking action.

5.1.3 Differences between drivers with different physiques

Finally, to compare the differences in pre-braking actions exhibited by subjects with different physiques, since some of the data does not fit the normal distribution, the Kruskal–Wallis test, one-way ANOVA test, and related post-hoc tests were used to analyze the data of IMF1 and IMF2's frequency and AMP.

Table 11 Results of Kruskal–Wallis ANOVA test for physique (average data)

Measure	Physique	<i>N</i>	Mean rank	Sig
Wf1	Phys.45	18	58.50	0.434
	Phys.50	65	48.69	
	Phys.55	17	48.94	
Kf1	Phys.45	18	51.89	0.526
	Phys.50	65	52.02	
	Phys.55	17	43.24	
Af1	Phys.45	18	49.44	0.363
	Phys.50	65	53.05	
	Phys.55	17	41.88	
Wa1*	Phys.45	18	40.33	0.002
	Phys.50	65	57.94	
	Phys.55	17	32.82	
Ka1*	Phys.45	18	43.78	0.011
	Phys.50	65	56.54	
	Phys.55	17	34.53	
Aa1‡	Phys.45	18	43.89	0.090
	Phys.50	65	55.09	
	Phys.55	17	39.94	
Wf2	Phys.45	9	26.89	0.828
	Phys.50	32	25.06	
	Phys.55	10	28.20	
Kf2	Phys.45	9	29.67	0.710
	Phys.50	32	25.03	
	Phys.55	10	25.80	
Af2	Phys.45	9	27.44	0.196
	Phys.50	32	27.97	
	Phys.55	10	18.40	
Wa2*	Phys.45	9	27.33	0.002
	Phys.50	32	30.16	
	Phys.55	10	11.50	
Ka2*	Phys.45	9	18.67	0.000
	Phys.50	32	32.78	
	Phys.55	10	10.90	
Aa2*	Phys.45	9	22.89	0.021
	Phys.50	32	30.12	
	Phys.55	10	15.60	

‡*p*-value < 0.1**p*-value < 0.05

For the average data, as shown in Table 11, for IMF1, significant differences ($p < 0.05$) were identified for the indicators Wa1 and Ka1 of IMF1 and the indicators Wa2, Ka2, and Aa2 of IMF2. Moreover, when the significance level was relaxed to 0.1 ($p < 0.1$), a significant difference was confirmed for Aa1.

As shown in Table 12, the results of post-hoc tests showed that for drivers with different physiques, a difference could only be confirmed between the Phys.50 and 55 levels. This means that drivers of Phys.50 may use a higher force than others on all joints (waist, knee, and ankle) for both sub-actions IMF1 and IMF2.

For the standard variance data, as shown in Table 13, significant differences ($p < 0.05$) were identified only for the indicator Kas2 of the IMF2. Moreover, when the significance level was relaxed to 0.1 ($p < 0.1$), a significant difference was also confirmed for Was2.

Similar to the results of the average data, based on the post-hoc tests for Kas2 (Table 14), the results indicate that the drivers at the Phys.55 level may have a significantly smaller knee vibration on AMP than the others for the sub-action of IMF2.

5.1.4 Summary and discussion

In summary, for both types of data about sub-action IMF1, the results showed significant differences for measures Af1 (for different driving experience), Ka1 (for different genders), and Wa1 and Ka1 (for different physiques). Because the IMF1 sub-actions were similar for almost all subjects in terms of speed and power, IMF1 can be indicated as the common and necessary main action when pre-braking.

The results showed that during pre-braking, the experienced drivers' ankle joint changing speed was slower than the novices, and female drivers may have had a higher force on their knee joint during the motion. Based on the results, one possible explanation is that the experienced drivers had enough anticipation of their future actions, so they moved their ankles more smoothly to maintain safety. Besides, the female drivers needed to use more force to move their lower legs via the knee joint to brake. Because braking is a common action in driving, this may cause female drivers to burn out faster while driving than males. Moreover, the related post-hoc tests for different physiques indicated similar results: the drivers that had Phys.50 needed to spend more force while pre-braking.

However, for sub-action IMF2, which existed only as part of drivers' pre-braking behaviors, the results were more complicated. For example, the results indicated that the experienced drivers had a higher score on the measures of kfs2 and kas2, which means that for the sub-action IMF2, the experienced drivers' knee joint's changing movements were heavier than for the novices. These results are consistent with our previous studies (Wu et al. 2020b) that during pre-braking, experienced drivers' foot movement distance was longer than the novice for safety (an experienced driver's

Table 12 Post-hoc test for Kas2 of IMF2 (average data)

	Sample 1-sample 2	Test statistic	Std. Error	Std. Test statistic	Sig	Adj. Sig
Wa1	Phys.55–Phys.45	7.510	9.812	0.765	0.444	1.000
	Phys.55–Phys.50*	25.115	7.903	3.178	0.001	0.004
	Phys.45–Phys.50	–17.605	7.727	–2.278	0.023	0.068
Ka1	Phys.55–Phys.45	9.248	9.812	0.943	0.346	1.000
	Phys.55–Phys.50*	22.009	7.903	2.785	0.005	0.016
	Phys.45–Phys.50	–12.761	7.727	–1.651	0.099	0.296
Aa1	Phys.55–Phys.45	3.948	9.812	0.402	0.687	1.000
	Phys.55–Phys.50‡	15.151	7.903	1.917	0.055	0.166
	Phys.45–Phys.50	–11.203	7.727	–1.450	0.147	0.441
Wa2	Phys.55–Phys.45‡	15.833	6.830	2.318	0.020	0.061
	Phys.55–Phys.50*	18.656	5.386	3.464	0.001	0.002
	Phys.45–Phys.50	–2.823	5.609	–0.503	0.615	1.000
Ka2	Phys.55–Phys.45	7.767	6.830	1.137	0.256	0.767
	Phys.55–Phys.50*	21.881	5.386	4.063	0.000	0.000
	Phys.45–Phys.50*	–14.115	5.609	–2.516	0.012	0.036
Aa2	Phys.55–Phys.45	7.289	6.830	1.067	0.286	0.858
	Phys.55–Phys.50*	14.525	5.386	2.697	0.007	0.021
	Phys.45–Phys.50	–7.236	5.609	–1.290	0.197	0.591

‡*p*-value < 0.1**p*-value < 0.05

foot is kept away from the pedals to ensure the pedals are not depressed by accident), so experienced drivers needed to move their foot to the brake pad with a higher speed.

Based on our assumptions about experienced drivers (i.e., experienced drivers are safer and rationalize their driving behaviors), it can be deduced from the results that the IMF2 sub-action may be a relatively necessary safety assurance action during pre-braking.

Besides, the results also indicate that female drivers had a higher score on the measure of Ka2, similar to the sub-action IMF1. This result confirmed our hypothesis once again that female drivers tend to burn out faster while driving than males.

In addition, similar to the results of sub-action IMF1, the related post-hoc results of IMF2 indicate that the drivers with Phys.50 had a higher score on the measures Wa2, Ka2, Aa2, and Kas2, than the other two physiques, especially for Phys.55. Given the results for drivers with different driving experience, the results for different physiques can be explained because drivers with Phys.50 may have more consistent driving behaviors than the others. One possible explanation is that the driving environment of vehicles was designed primarily for divers of average size.

Therefore, in order to better explain these results, in particular to explain the results of IMF2, the motion data of subjects were compared and analyzed specifically using HHT spectra.

5.2 Graph-based Comparative Analysis

As described in Sect. 3.1, this paper focused only on the pre-braking part of the whole braking actions of the drivers. Unlike the statistical analysis, which did not take into account time, before analyzing the pre-braking actions' HHT spectrum with time attributes, we first determined its time-relationship with the braking action of drivers.

First, we extracted the coordinates data of one driver's tiptoe during the pre-braking action and depicted in Fig. 7 its height change trajectory on the z-axis. This driver's movements typically took about 6 s. In Fig. 7a, we can clearly see that the driver's tiptoe action during the pre-braking action went through a process of raising, reaching the peak, starting to land, and then touching the brake plate. The green dotted line shows the approximate area where the toe moves to its highest point, and the red dotted line shows the approximate point at which the pre-braking action ends.

Meanwhile, to facilitate comparison, we standardized the data for different lengths of time and resampled all motion samples to 0.65 s (average time) using linear interpolation. As the result, we calculated the average HHT spectrum for waist, knee, and ankle from all collected data (Fig. 7b–d). To compare these spectra by each group, the amplitudes of waist, knee, and ankle were set to 0~0.1 degrees, 0~0.5 degrees, and 0~2.0 degrees, respectively, because these ranges were appropriate enough to investigate the features among the three groups.

Table 13 Results of Kruskal–Wallis ANOVA test for physique (standard variance data)

Measure	Physiques	N	Mean rank	Sig
Wfs1	Phys.45	18	50.33	0.991
	Phys.50	65	50.75	
	Phys.55	17	49.71	
Kfs1	Phys.45	18	52.83	0.800
	Phys.50	65	50.89	
	Phys.55	17	46.53	
Afs1	Phys.45	18	51.33	0.852
	Phys.50	65	49.42	
	Phys.55	17	53.76	
Was1	Phys.45	18	45.89	0.275
	Phys.50	65	53.85	
	Phys.55	17	42.59	
Kas1	Phys.45	18	55.94	0.275
	Phys.50	65	51.51	
	Phys.55	17	40.88	
Aas1	Phys.45	18	54.67	0.729
	Phys.50	65	48.89	
	Phys.55	17	52.24	
Wfs2	Phys.45	9	23.67	0.454
	Phys.50	32	27.97	
	Phys.55	10	21.80	
Kfs2	Phys.45	9	32.11	0.271
	Phys.50	32	25.81	
	Phys.55	10	21.10	
Afs2	Phys.45	9	29.33	0.751
	Phys.50	32	25.09	
	Phys.55	10	25.90	
Was2‡	Phys.45	9	30.00	0.090
	Phys.50	32	27.72	
	Phys.55	10	16.90	
Kas2*	Phys.45	9	24.67	0.27
	Phys.50	32	29.72	
	Phys.55	10	15.30	
Aas2	Phys.45	9	27.22	0.523
	Phys.50	32	27.16	
	Phys.55	10	21.20	

‡p-value < 0.1

*p-value < 0.05

By calibrating the end time (red dashed line, meaning the foot touched the brake pad at about 0.6 s) of tiptoe action and HHT spectra, the results showed that the values of AMP were weaker (bluer) than others in the time period of 0.3 to 0.5 s (green dashed lines) in all HHT spectra, and the time period just coincided with the time period where the subject's tiptoe reached the peak (the curve flattened out).

These results may indicate that most drivers tend to diminish the forces used by their waist, ankle, and knee when the foot reaches the peak. Although each driver took slightly different amounts of time to do the pre-braking movements, the feature of time period from 0.3 to 0.5 s in the figure can be considered as a sign that a driver's foot has reached the longitudinal peak point, which provided an important reference for the next analysis of the meaning of the various IMF sub-actions. In this study, we defined the time period from about 0.1 to 0.6 s as the main period, and the time period from 0.3 s to 0.5 s as the P period.

5.2.1 Sub-actions IMF1 and IMF2

Because the target IMF1 and IMF2 existed in the complex spectrum, we extracted them separately for the analysis at first. Figure 8 describes the average spectrum of IMF1 for the joints of waist, knee, and ankle.

As shown in Fig. 8, IMF1 had a relatively smooth frequency curve for all joints (waist, knee, and ankle), and during the main time period (about 0.1 ~ 0.6 s, including P period), its AMP showed a gentle decreasing trend. Because the frequency can represent the action speed and AMP can represent the force used, IMF1 fits our understanding of general pre-braking behaviors (uniform speed, AMP becomes smaller). These results may mean that the sub-action IMF1 may represent the basic action in whole pre-braking behaviors (raising the right foot to the brake plate; regular actions a, b, and c in Fig. 1).

However, compared to sub-action IMF1, sub-action IMF2 had a higher frequency, which may mean that the action represented by IMF2 was redundant or contained/involved assistant actions that were distinct from the basic action.

As shown in Fig. 9, IMF2 had a more oscillating curve than IMF1, which was characterized by a wave peak in P

Table 14 Post-hoc test for Kas2 of IMF2 (standard variance data)

	Sample 1-sample 2	Test statistic	Std. Error	Std. Test statistic	Sig	Adj. Sig
Kas2	Phys.55–Phys.45	9.367	6.830	1.371	0.170	0.511
	Phys.55–Phys.50*	14.419	5.386	2.677	0.007	0.022
	Phys.45–Phys.50	-5.052	5.609	-0.901	0.368	1.000

‡p-value < 0.1

*p-value < 0.05

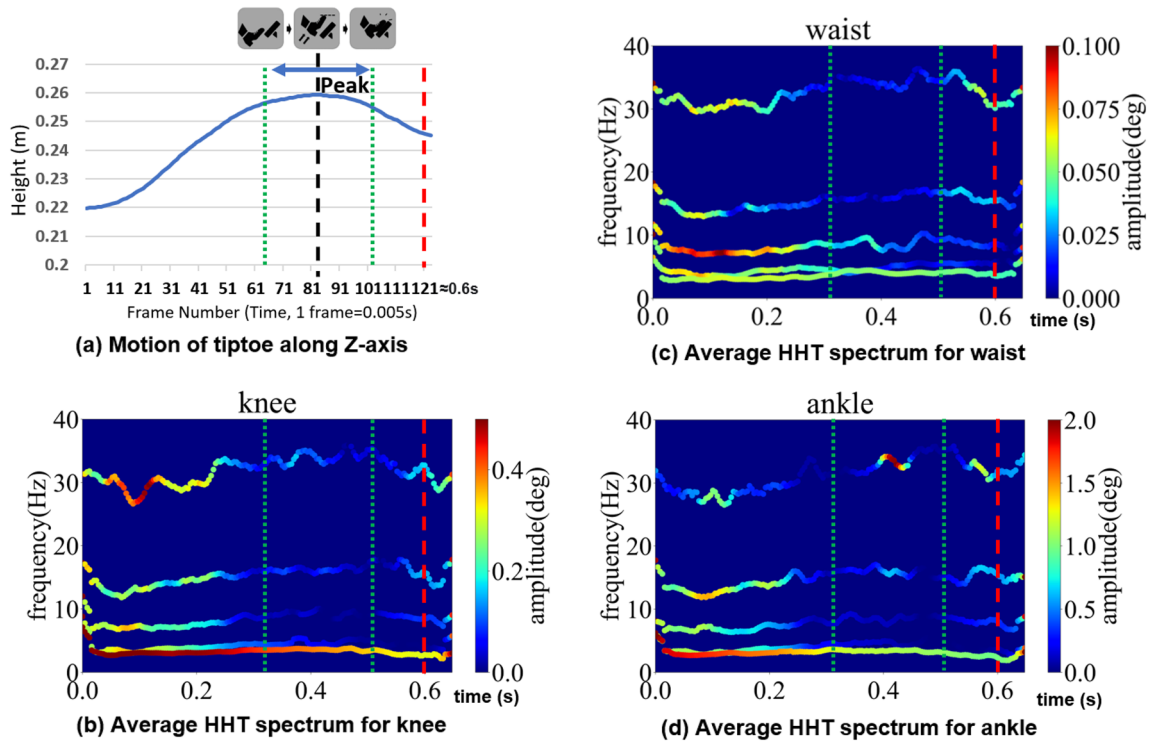


Fig. 7 Results of tiptoe motion and HHT spectra for waist, knee, and ankle

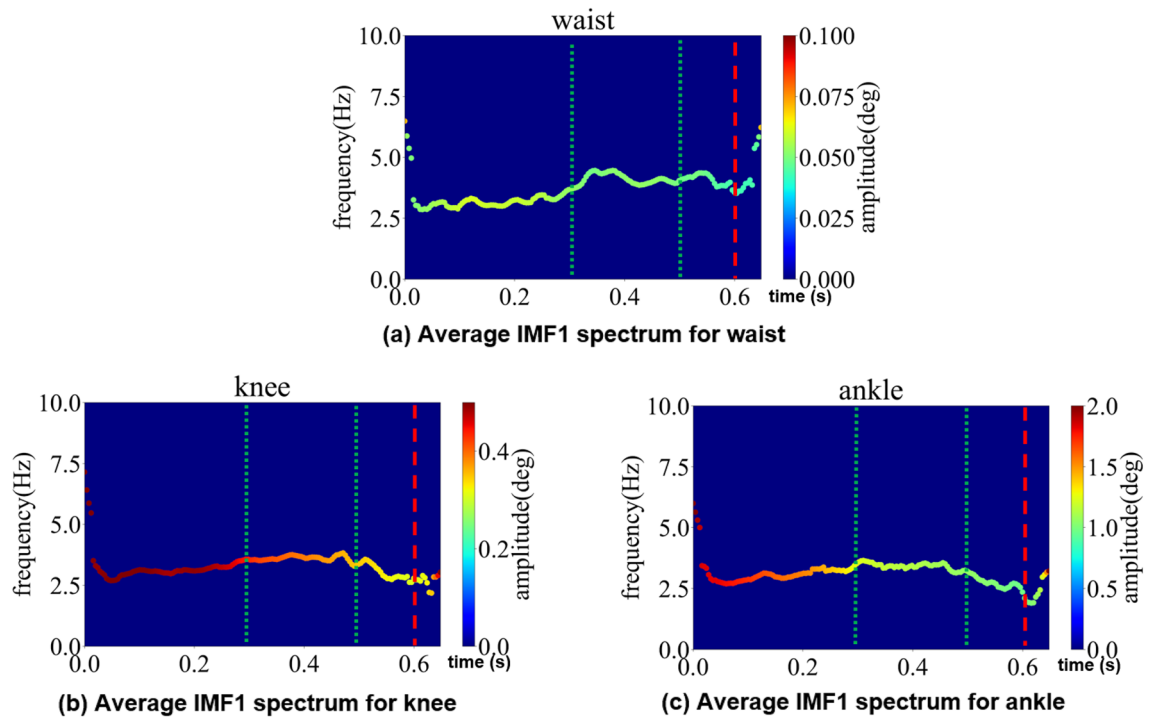


Fig. 8 Results of average IMF1 spectrum for waist, knee, and ankle during pre-braking

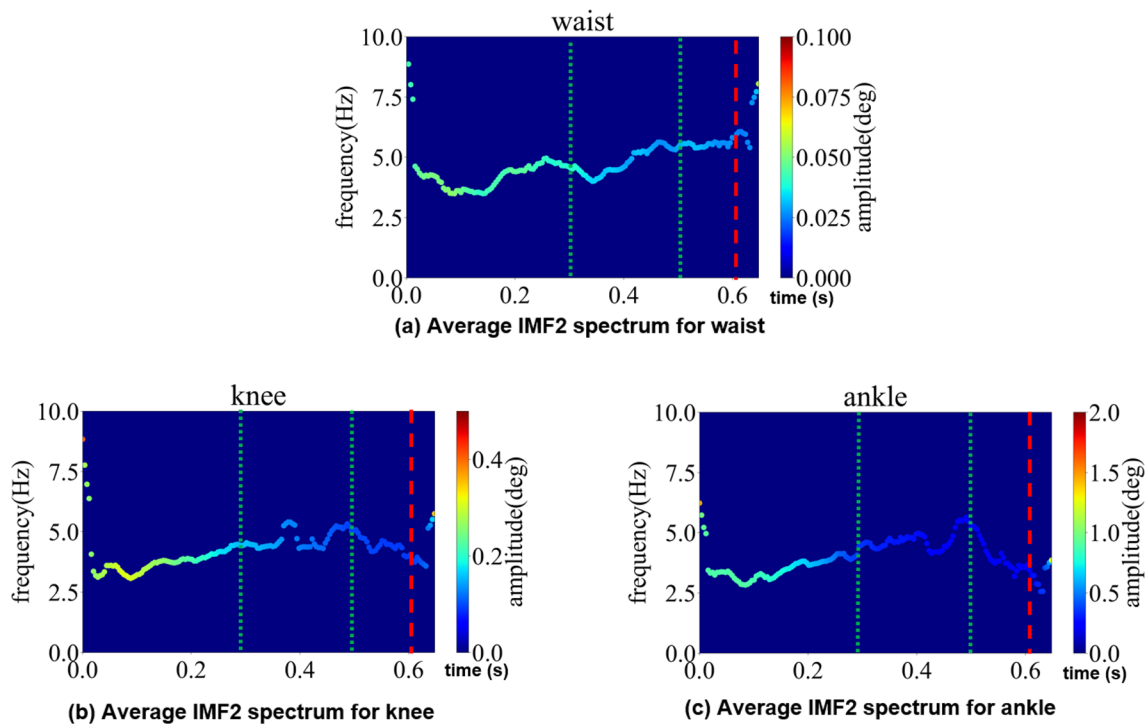


Fig. 9 Results of average IMF2 spectrum for waist, knee, and ankle during pre-braking

period (for knee and ankle), which means that the IMF2 sub-actions in P period would experience a process of surge and decrease in speed. Meanwhile, compared with IMF1, we also found that its AMP presented a drastically decreasing trend, and the stronger AMP occurred outside the P period (focus on the front), which could mean that the actions represented by IMF2 occurred mainly during the lift phase of the subject's foot. Combined with the results of statistical analysis and the conclusions of our previous research (Wu et al. 2020b), we speculate that IMF2 represents the transverse movement of the driver's foot. As a safety precaution, some drivers keep their feet as far away from the brake pad as possible. This results in significant lateral foot movement during braking.

However, according to the statistical analysis results of Sect. 5.1, some statistical differences were found between the different groups. Therefore, in order to validate our discussion of the results and to better analyze the differences found in Sect. 5.1, we compared the IMF1 and IMF2's graphs of different groupings.

5.2.2 Graph comparative analysis of IMF1

As shown in Fig. 10, all drivers performed the IMF1 sub-action. Based on the results of statistical analysis for different driving experience of sub-action IMF1 (Novice > Exp. for Af1), we confirmed that the results in the graph were consistent with our previous conclusions. The results mainly showed that after P period, novice drivers tended to drop their foot more quickly, which is consistent with the results of our previous research (Wu et al. 2020b). In addition, by comparing the AMPs of each graph, we can determine that the novice drivers were more inclined to counterbalance the force used throughout the pre-braking process, rather than being as focused as the experienced driver.

Similar situations were found for different genders. As shown in Fig. 11, based on the results of statistical analysis of different genders for sub-action IMF1 (Female > Male for Ka1), the difference in the graph for the main time period was confirmed, especially before P period. In addition, by comparing the graphs, we found that the curve of the male

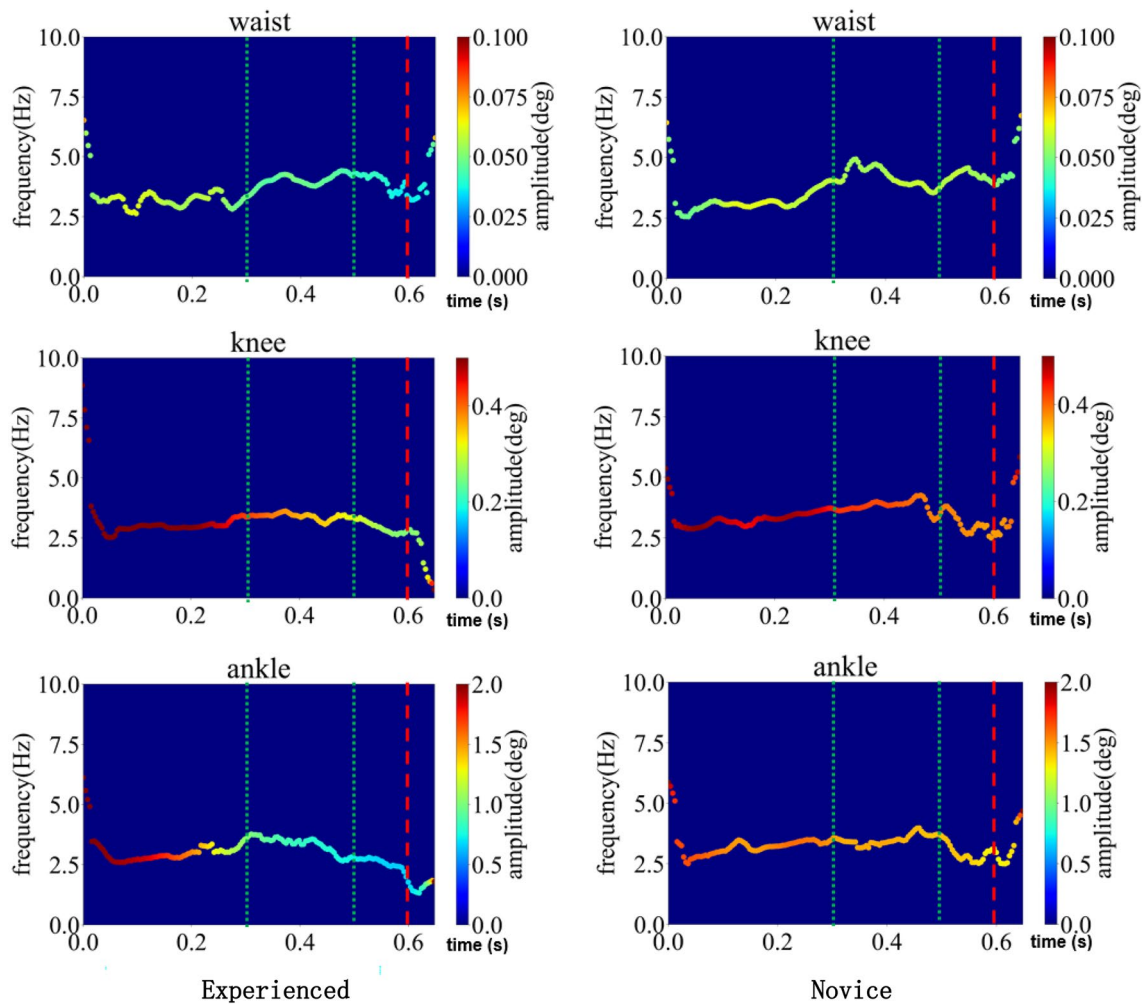


Fig. 10 Results of graph comparative analysis with different driving experience for IMF1

was relatively smoother, which means that the speed change of the female knee joint was more drastic during the pre-braking process.

Moreover, As shown in Fig. 12, based on the results of statistical analysis of different genders for sub-action IMF1 (Phys.50 > Phys.55 for Wa1 and Ka1), the significant difference of AMP can easily be confirmed on the graphs. In addition, we also found among the graphs, that Phys.50 may have the highest performance for AMP during the main time period.

In summary, for the sub-action IMF1 of pre-braking behaviors, in addition to identifying some differences in AMPs (shown in Sect. 5.1), there were no significant differences between groups in other measures. The results were in line with our expectation for IMF1 (a basic action of

pre-braking). However, some differences for AMPs were big enough to be considered in future assisted driving designs.

5.2.3 Graph comparative analysis of IMF2

Only some of drivers may perform the IMF2 sub-action, based on the statistical analysis of different driving experiences for sub-action IMF2 (Exp. > Novice for Kfs2 and Kas2). As shown in Fig. 13, we confirmed that the results in the graph were consistent with our previous conclusion. Similar to the results of IMF1, the experienced drivers' frequencies changed more smoothly, and their AMP values were stable and showed a decreasing trend.

Next, as shown in Fig. 14, based on the statistical analysis of different genders for sub-action IMF2 (Female > Male

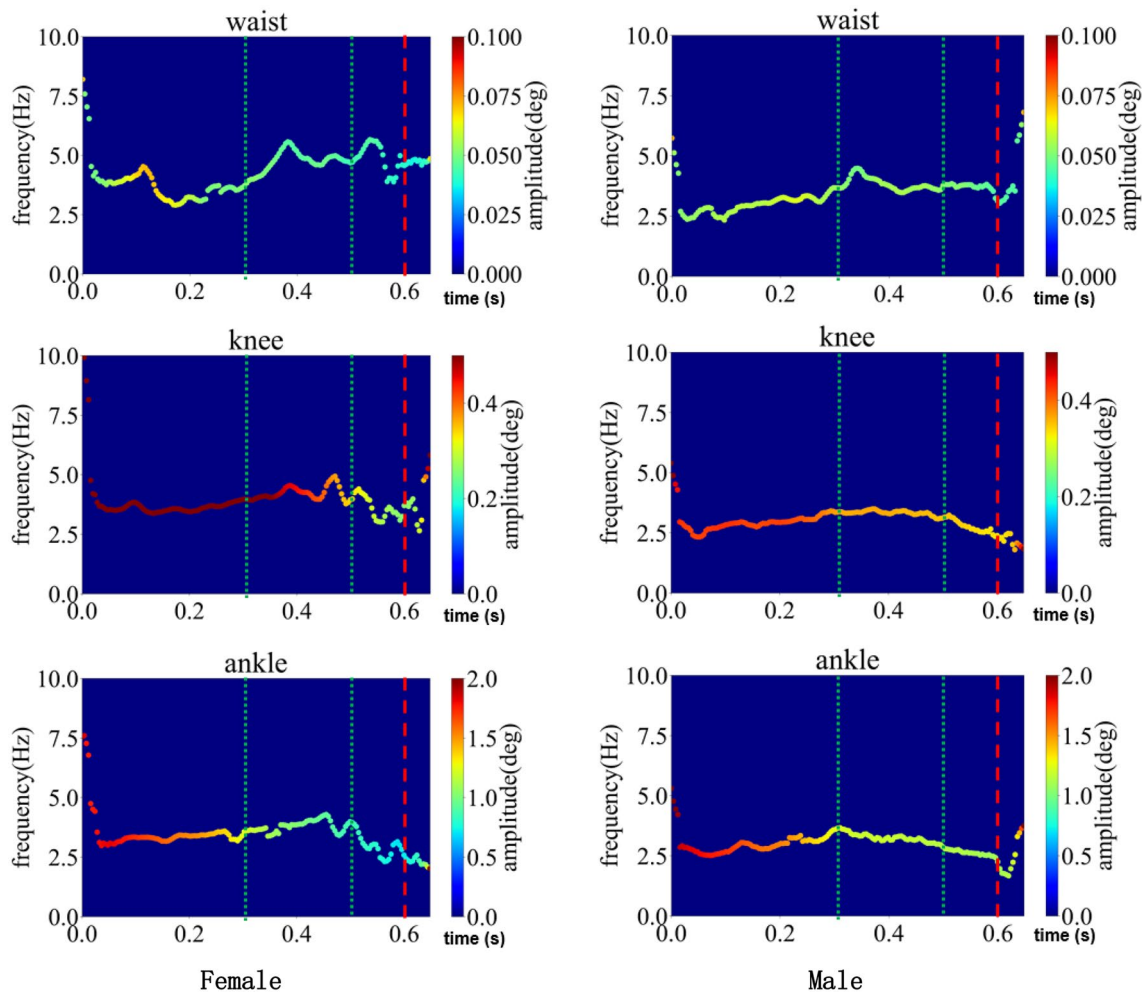


Fig. 11 Results of graph comparative analysis with different gender for IMF1

for Ka2), we found that significantly higher AMP values of females mainly occurred before P period, which was consistent with our previous discussion. In addition, we found that the frequency curve was smoother for men and experienced drivers.

Finally, as shown in Fig. 15, based on the statistical analysis of different physiques for sub-action IMF2 (Phys.50 > Phys.55 for Wa2, Ka2, Aa2, and Kas2), we confirmed the same difference in the graphs, which supported the discussion in the previous section. In addition, similar to the results for IMF1, we confirmed that Phys.50 may have the highest performance for AMP during the main time period. Moreover, by comparing all the plots, we found that Phys.50, as well as men and experienced drivers, had the smoothest frequency curve.

In summary, for the sub-action IMF2 of pre-braking behaviors, we confirmed most of the differences at the AMP

level, which confirmed our discussion results in Sect. 5.1. Moreover, we found a pattern that some groups (experienced drivers, males, Phys.50) had smoother frequency curves and their AMP decreased at a constant rate. Based on the assumption that experienced drivers behave more efficiently, we conclude that males and Phys.50 drivers may have performed relatively better under the current experimental conditions.

The related results demonstrate that a good driving environment needs to be fine-tuned according to the individual elements (driving experiments, gender and physique, etc.) of the specific driver. Which means that the findings of this study can provide data to support future assisted driving systems that automate the adjustment of the driving environment and apply the personalized training of novice drivers in the future.

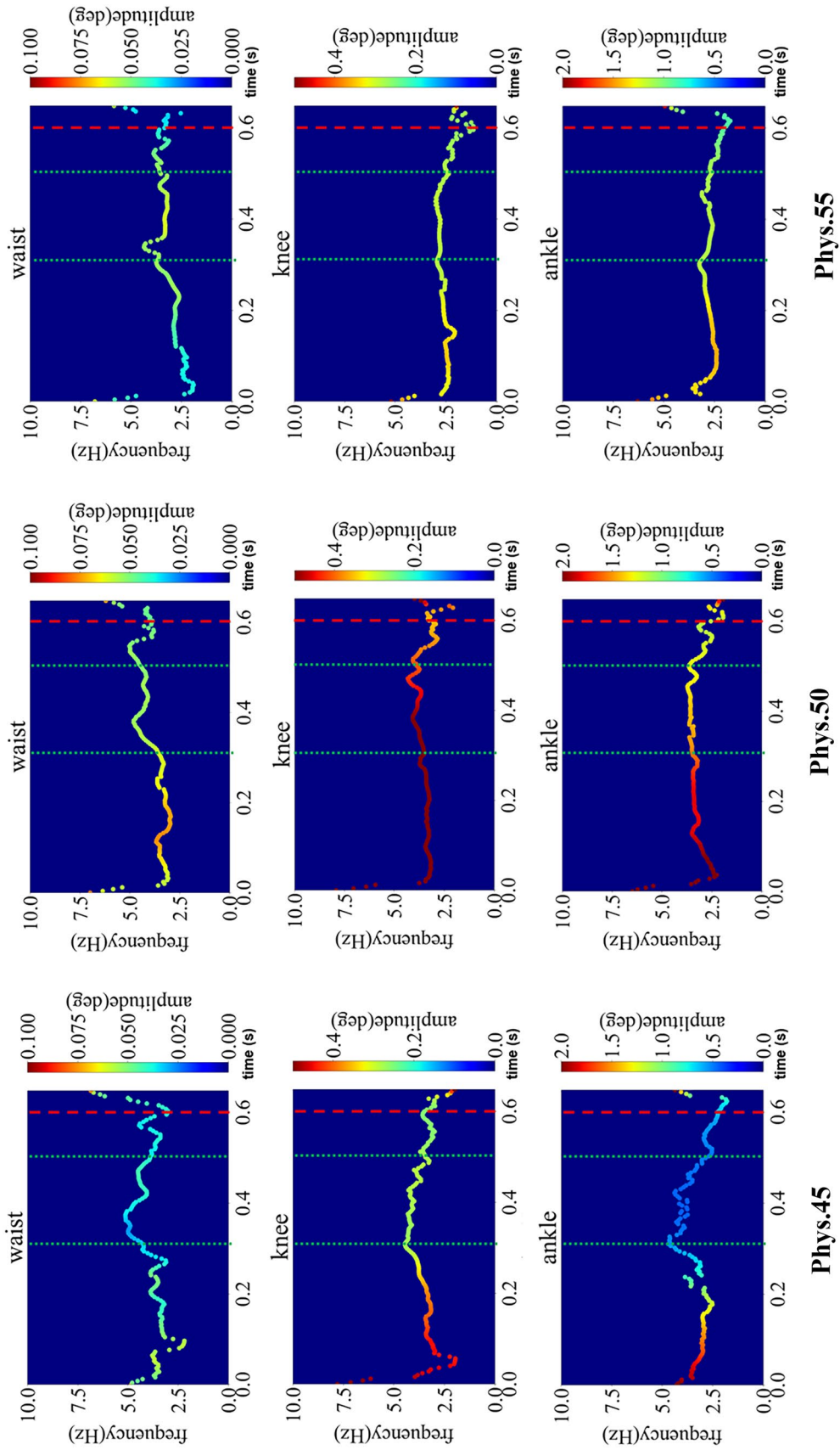


Fig. 12 Results of graph comparative analysis of different physiquises for IMF1

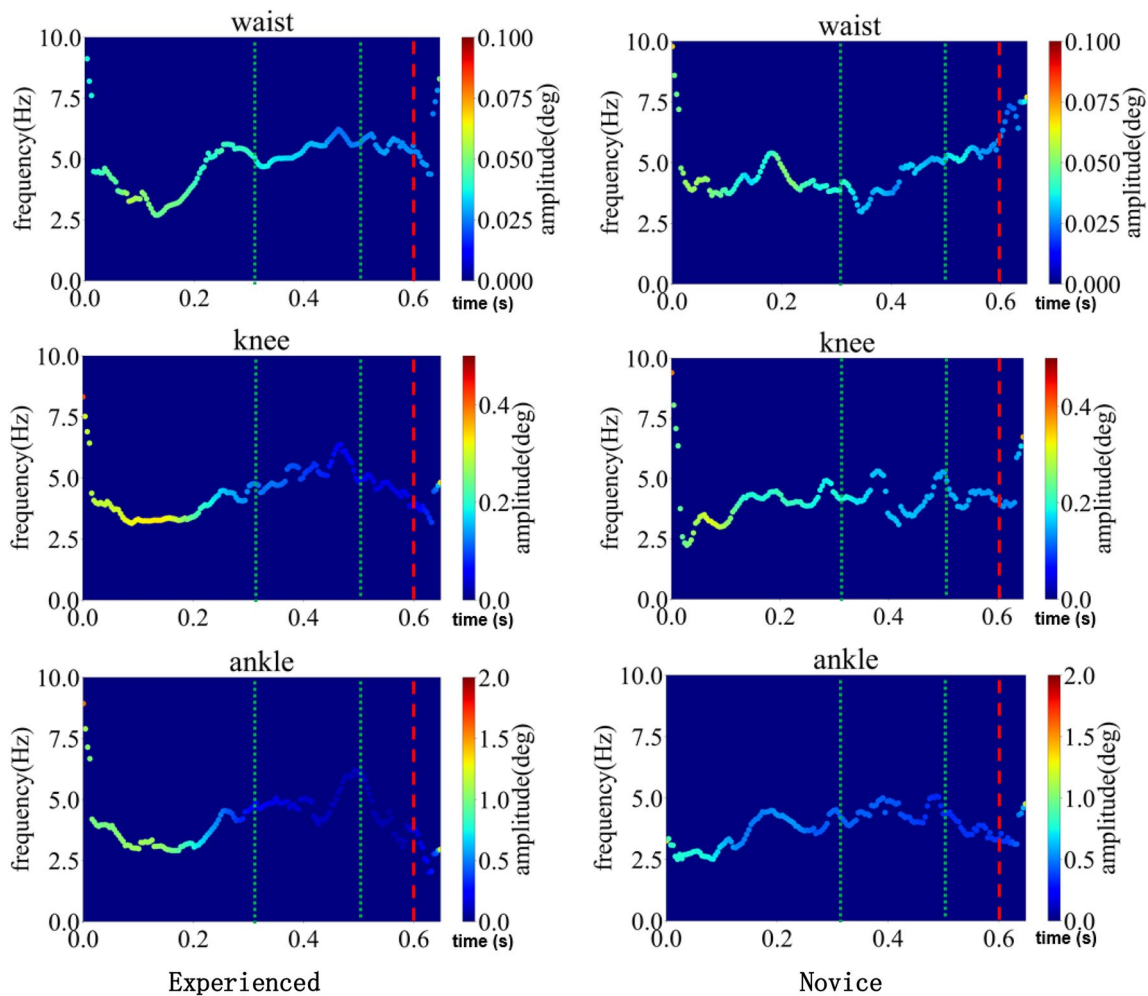


Fig. 13 Results of graph comparative analysis with different driving experience for IMF2

6 Conclusion

To discover similarities and differences in pre-braking behaviors among drivers with different driving experience, genders, and physiques, this study analyzed drivers' pre-braking related local body joints movements by using a motion capture device and provided a Hilbert–Huang Transform (HHT)-based local human body movement analysis method to decompose the realistic complex pre-braking actions into many sub-actions by their frequencies.

Based on the results of angle analysis for 50 sets of experimental motion data collected from 10 drivers, the

Hilbert–Huang Transform method found two important sub-actions during pre-braking: IMF1 and IMF2.

For these two sub-actions, based on related statistical analyses, the results showed that sub-action IMF1 may be the common and necessary action during pre-braking and sub-action IMF2 is a relatively necessary safety assurance action during pre-braking, because only some drivers performed the IMF2 sub-action. Based on this, we verified that IMF2 was the right foot transverse movement at the beginning part of the pre-braking process, which confirmed our previous work (Wu et al. 2020b).

Based on the graph-based comparative analysis and the assumption that experienced drivers behave more efficiently,

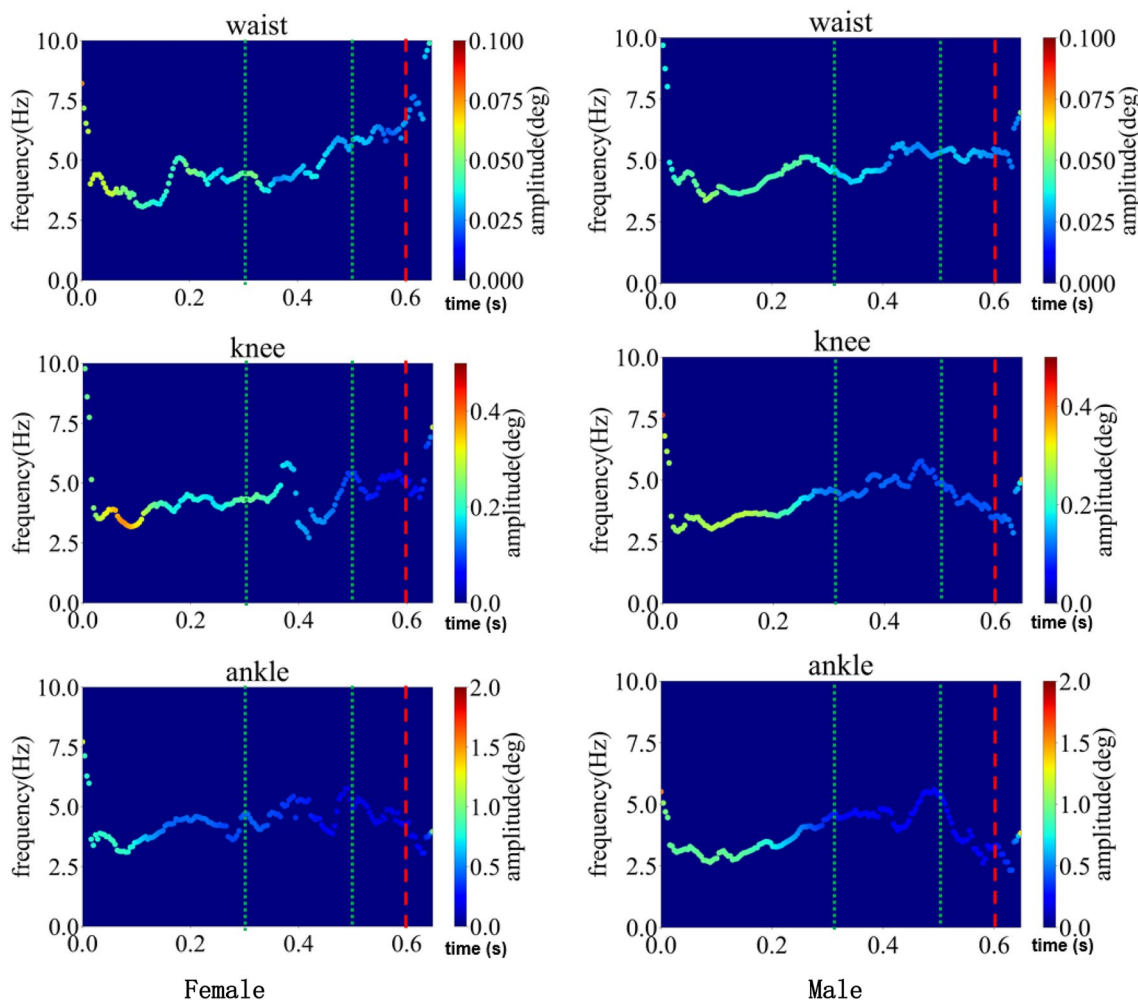


Fig. 14 Results of graph comparative analysis of different genders for IMF2

we found that some groups (experienced, males, Phys.50) had consistent characteristics (smoother frequency curves and uniformly decreasing AMP values), which could mean that in this experimental environment, such drivers would have better performance and efficiency. For example, female drivers may tend to use more force to perform braking actions. Moreover, existing models of vehicles may be designed for people of medium size (Phys.50), so additional designs or devices may be necessary for drivers of other sizes. These results can be applied to the individualized training of new drivers and the development of related assistance systems in the future.

This study, which examined the differences in body movements during pre-braking between drivers with different characteristics, had some limitations: 1) for reasons of time and equipment, the sample size of 100 was small; 2) this study was merely explorative, and the statistical results may not to be taken as confirmatory.

In future work, we plan to conduct more relevant experiments and consider additional elements to enrich the driver behavior model. Moreover, we plan to collectively analyze eye-tracking data and motion capture data to determine the relationship between drivers' eye movements and body movements during braking.

Acknowledgements The authors wish to thank all the workers who participated in the experiments. Co-first author: Yishui Zhu; Corresponding authors: Ran Dong. On behalf of all authors, the corresponding author states that there is no conflict of interest.

Funding This research was funded by JSPS KAKENHI [grant numbers JP21K11876, JP21K17833].

Availability of data and materials The data will be made available upon request.

Declarations

Conflict of interest The authors declare that they have no competing interests.

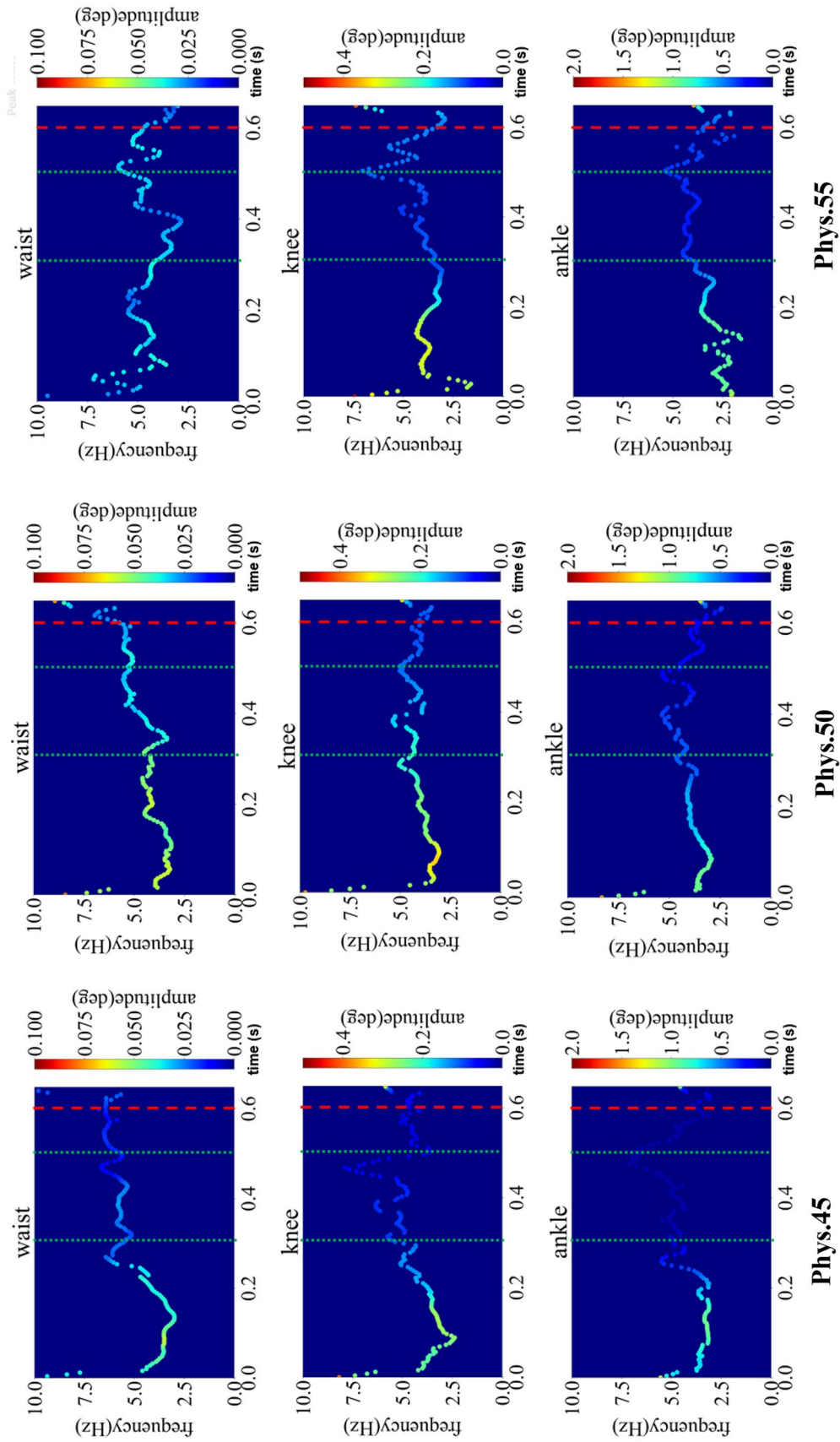


Fig. 15 Results of graph comparative analysis of different physiques for IMF2

Open Access This article is licensed under a Creative Commons Attribution 4.0 International License, which permits use, sharing, adaptation, distribution and reproduction in any medium or format, as long as you give appropriate credit to the original author(s) and the source, provide a link to the Creative Commons licence, and indicate if changes were made. The images or other third party material in this article are included in the article's Creative Commons licence, unless indicated otherwise in a credit line to the material. If material is not included in the article's Creative Commons licence and your intended use is not permitted by statutory regulation or exceeds the permitted use, you will need to obtain permission directly from the copyright holder. To view a copy of this licence, visit <http://creativecommons.org/licenses/by/4.0/>.

References

- Aminian, K., Najafi, B.: Capturing human motion using body-fixed sensors: outdoor measurement and clinical applications. *Comput. Anim. Virtual Worlds*. **15**(2), 79–94 (2004)
- Bracewell, R.N.: *Fourier transform and its applications*. McGraw-Hill Inc Press, Location (1978)
- Bruderlin, A., Williams, L., 1995. Motion signal processing. Proceedings of the 22nd Annual Conference on Computer Graphics and Interactive Techniques.
- Cao, S., et al.: Effect of driving experience on collision avoidance braking: an experimental investigation and computational modelling. *Behav. Inf. Technol.* **33**(9), 929–940 (2014)
- Dong, R., Chen, Y., Cai, D., Nakagawa, S., Higaki, T., Asai, N.: Robot motion design using Bunraku emotional expressions—focusing on Jo-Ha-Kyū in sounds and movements. *Adv. Robot.* **34**(5), 299–312 (2020a)
- Dong, R., Dongsheng, C., Soichiro, I.: Motion capture data analysis in the instantaneous frequency-domain using Hilbert-Huang transform. *Sensors* **20**(22), 6534 (2020b)
- Dong, R., Qiong C., Soichiro I., 2021. A deep learning framework for realistic robot motion generation. *Neural Comput. Appl.* 1–14.
- Hault-Duburle, A., Robache, F., Pacaux, M.P., Morvan, H.: Determination of pre-impact occupant postures and analysis of consequences on injury outcome. Part I: a driving simulator study. *Accid. Anal. Prev.* **43**(1), 66–74 (2011)
- Hou, L., Duan, J., Wang, W., Li, R., Li, G., Cheng, B.: Drivers' braking behaviors in different motion patterns of vehicle-bicycle conflicts. *J. Adv. Transp.* **2019**, 17 (2019)
- Huang, N.E., Shen, S.P.S.: *Hilbert-Huang transform and its applications*, vol. 16. World Scientific, Singapore (2014)
- Jia, S., et al.: Long short-term memory and convolutional neural network for abnormal driving behaviour recognition. *IET Intel. Transport Syst.* **14**(5), 306–312 (2020)
- Li, Y., et al., 2017. Braking assistance algorithm considering driver characteristics at signalized intersection. 4th International Conference on Transportation Information and Safety (ICTIS). Banff, Canada.
- Li, H., et al.: Characteristics of vehicle spatiotemporal diagram under the emergency braking warning. *J. South China Univ. Technol. (natural Science Edition)*. **48**(7), 76–84 (2020). ((in Chinese))
- Lodha, N., et al.: Cognitive and motor deficits contribute to longer braking time in stroke. *J. Neuroeng Rehabil.* **18**, 1–10 (2021)
- Lyu, N., Xie, L., Wu, C., Fu, Q., Deng, C.: Driver's cognitive workload and driving performance under traffic sign information exposure in complex environments: a case study of the highways in China. *Int. J. Environ. Res. Public Health.* **14**, 203 (2017)
- Lyu, N., Cao, Y., Wu, C., Xu, J., Xie, L.: The effect of gender, occupation and experience on behavior while driving on a freeway deceleration lane based on field operational test data. *Accid. Anal. Prev.* **121**, 82–93 (2018)
- National Highway Traffic Safety Administration (NHTSA), 2002. Traffic safety facts 2002. Technical report. U.S. Department of Transportation.
- Nugroho, H.S., M.A. Dewantoro, Anindito A., 2021. Android and cloud-based application development to predict remaining age of four-wheeled vehicle brake pad with varied driving behaviour. *IOP Conference Series: Materials Science and Engineering*. 1116.
- Pawar, N.M., et al.: Modelling braking behaviour and accident probability of drivers under increasing time pressure conditions. *Accid. Anal. Prev.* **136**, 105401 (2020)
- Rehman, N., Mandic, D.P.: Multivariate empirical mode decomposition. *Royal Soc.* **466**, 1291–1302 (2010)
- Ren, Y., Li J., Yan, G., Wang, W., Liu, X., Zhang, J., 2011. Modeling of the Chinese driver's braking behavior in the simulated traffic scene of rear-end collision avoidance. 7th Advanced Forum on Transportation of China (AFTC 2011). Beijing. 92–97.
- Rongqiang, G., Jian, F., Junyi, L., 2016. Based on binocular identification technology of automobile active braking safety distance model research. 2016 International Symposium on Computer, Consumer and Control (IS3C), Xi'an. 355–357.
- RxKinetics, 2020. Estimating height in bedridden patients, software solutions for pharmacists. http://www.rxkinetics.com/height_estimate.html (Accessed 17 Sept 2020).
- Schmidt, R.A., Young, D.E., Ayres, T.J., Wong, J.R., 1997. Pedal misapplications: their frequency and variety revealed through police accident reports. Proceedings of the Human Factors and Ergonomics Society Annual Meeting. SAGE Publications, Los Angeles, CA. 41(2).
- Stahl, P., Donmez, B., Jamieson, G.A.: Anticipation in driving: the role of experience in the efficacy of pre-event conflict cues. *IEEE Trans. Human-Machine Syst.* **44**(5), 603–613 (2014)
- Stavarakaki, A.M., et al.: Estimating the necessary amount of driving data for assessing driving behavior. *Sensors*. **20**(9), 2600 (2020)
- Susumu, E., Zama, Y., Ono, K., 2009. Prediction of pre-impact occupant kinematic behavior based on the muscle activity during frontal collision. *Engineering*.
- Thorpe, S., Fize, D., Marlot, C.: Speed of processing in the human visual system. *Nature* **381**, 520–522 (1996)
- Troje, N.F.: Decomposing biological motion: a framework for analysis and synthesis of human gait patterns. *J. vis.* **2**(5), 2–2 (2002)
- Tu, H., et al., 2015. Effects of driving simulator fidelity on the driving behavior of emergency braking. In: *New Frontiers in Road and Airport Engineering*. Shanghai, China.
- Winter, D.A.: *Biomechanics and motor control of human movement*. John Wiley & Sons, Location (2009)
- Wu, B., Zhu, X., Shen, J.: Driver emergency braking behavior based on naturalistic driving data. *J. Tongji Univ. Nat. Sci.* **46**(11), 1514–1519 (2018). ((in Chinese))
- Wu, B., Wu, Y., Aoki, Y., Nishimura, S.: Mowing patterns comparison: analyzing the mowing behaviors of elderly adults on an inclined plane via a motion capture device. *IEEE Access.* **8**, 216623–216633 (2020a)
- Wu, B., Zhu, Y., Nishimura, S., Jin, Q.: Analyzing the effects of driving experience on prebraking behaviors based on data collected by motion capture devices. *IEEE Access.* **8**, 197337–197351 (2020b)
- Xiao, J., Weng, Y., Xie, Y., 2019. Study on the prediction of driving braking behaviour based on FPN. 3rd Annual International

Conference on Cloud Technology and Communication Engineering (CTCE). Wuhan, China.

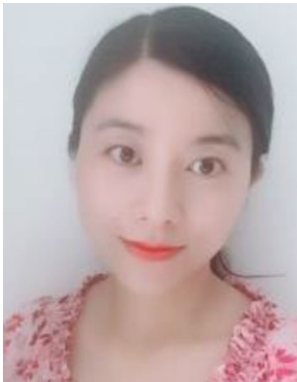
Xsens, 2022. Xsens MVN User manual, Xsens 3D motion tracking. https://www.xsens.com/hubfs/Downloads/usermanual/MVN_User_Manual.pdf (Accessed 1 Feb 2022).

Zhu, B., et al.: Personalized control strategy of electronic brake booster with driving behaviors identification. *IEEE Trans. Veh. Technol.* **70**(12), 12593–12603 (2021)



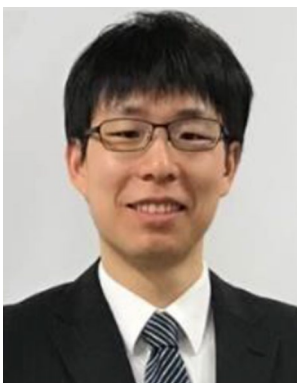
Bo Wu received the Ph.D. degree in Human Sciences from Waseda University, Tokyo, Japan in 2015. He is currently an assistant professor in the School of Computer Science of Tokyo University of Technology, Japan. He also is a Research Fellow with the Kansai University, DS lab. He has been engaged in the research fields of Internet of Things (IoT), information and computer science, and social and human informatics. His current research interests include human motion capture, eye-movement

analysis, machine learning & Big data analysis, and human-centered application system development. Dr. Wu is a member of IEEE CS and Information Processing Society of Japan.



Yishui Zhu received the Ph.D. degree in Human Sciences from Waseda University, Saitama, Japan in 2012. She is currently an Associate Professor of the Department of Software Engineering, School of Information Engineering, Chang'an University, Xi'an, China. She has been interested extensively in research works in the fields of service computing, network information systems, and human informatics, traffic services system. She seeks to exploit the rich interdependence between theory and practice

in her work with interdisciplinary and integrated approaches. Her recent research interests cover human-centric ubiquitous computing, traffic services, block-chain, behavior and cognitive informatics, big data, personal study behavior analytics and individual modeling. Dr. ZHU is a member of IEEE CS and ACM USA, CCF and Yocsef China.



Ran Dong obtained his Ph.D. degree in Engineering, the major of Computer Science from the Graduate school of Systems and Information Engineering of the University of Tsukuba in 2020. He is currently an assistant professor in the School of Computer Science of Tokyo University of Technology, Japan. His research centered on human-machine interaction, numerical simulation, and data analysis. Ran Dong has published his works in

international journals such as *Advanced robotics*, *Neural Computing, Applications*, *Sensors*, *Scientific Reports*. He also published his works in international conferences such as SIGGRAPH Talks and CGI in ACM Conference Proceedings. He is currently working on projects relating to robotic motion design, electromagnetic wave simulation, and motion analysis.



Kiminori Sato B.E, M.E and Ph.D. from Tohoku University, Japan in 1984, 1986 and 1989 respectively. Join Kagoshima University, Japan in 1989 as a research Associate at department of electrical engineering and was promoted to Professor in 2013. Currently a Professor at School of Computer Science, Tokyo University of Technology, Japan since 2019. Area of research interest are biometrics, computer vision and pattern analysis. Main professional membership includes member of IEICE, IPSJ

and etc.



Soichiro Ikuno School of Computer Science, Tokyo University of Technology, Tokyo, Japan. He received the B.E. and M.E. degrees in electrical and information engineering from Yamagata University, Yamagata, Japan, in 1994 and 1996, respectively, and the Ph.D. degree in information engineering from the University of Tsukuba, Tsukuba, Japan, in 1999. In 1999, He joined the Faculty of Engineering, Tokyo University of Technology, Tokyo, Japan, where he is currently a Professor

in the School of Computer Science. His research interest is in the numerical analysis of electromagnetic analysis and high performance computing.



Shoji Nishimura is a professor at Waseda University, Tokyo, Japan. His current research interests include educational technology, especially education and the Internet. He received his bachelor's degree in mathematics from Waseda University, MSc in applied physics from Waseda University, and PhD in Human Sciences from Osaka University. In 1991, he joined the Advance Research Center, INES Corporation as a senior researcher. Then, he joined the School of Human

Sciences, Waseda University, as an assistant professor in 1997. Currently, he is a professor in Faculty of Human Sciences, Waseda University. He is a member of Japan Society for Educational Technology, Japanese Society for Information and Systems in Education, and Information Processing Society of Japan.



Qun Jin received the Ph.D. degree in electrical engineering and computer science from Nihon University, Tokyo, Japan in 1992. He is currently a tenured Full Professor and the Chair of the Department of Human Informatics and Cognitive Sciences, Faculty of Human Sciences, Waseda University, Saitama, Japan. He has been engaged extensively in research works in the fields of computer science, information systems, and social and human informatics. He seeks to exploit the rich

interdependence between theory and practice in his work with interdisciplinary and integrated approaches. His recent research interests

cover human-centric ubiquitous computing, human–computer interaction, behavior and cognitive informatics, big data, personal analytics and individual modeling, MOOCs and learning analytics, and computing for well-being. Prof. Jin is a member of IEEE CS and ACM USA; IEICE, IPSJ, and JSAI Japan; and CCF China.